JOURNAL OF VIROLOGY, Sept. 2009, p. 8514–8524 Vol. 83, No. 17
0022-538X/09/$08.00+0 doi:10.1128/JVI.00785-09

Epigenetic Modulation of Gene Expression from Quiescent Herpes Simplex Virus Genomes▽

Michael W. Ferenczy and Neal A. DeLuca*

Department of Microbiology and Molecular Genetics, University of Pittsburgh School of Medicine, Pittsburgh, Pennsylvania 15261

Received 17 April 2009/Accepted 20 May 2009

The ability of herpes simplex virus to persist in cells depends on the extent of viral-gene expression, which may be controlled by epigenetic mechanisms. We used quiescent infection with the viral mutants d109 and d106 to explore the effects of cell type and the presence of the viral protein ICP0 on the expression and chromatin structure of the human cytomegalovirus (HCMV) tk and gC promoters on the viral genome. Expression from the HCMV promoter on the d109 genome decreased with time and was considerably less in HEL cells than in Vero cells. Expression from the HCMV promoter in d106 was considerably more abundant than in d109, and this increased with time in both cell types. The same pattern of expression was seen on the tk and gC genes on the viral genomes, although the levels of tk and gC RNA were approximately 10^2- and 10^5-fold lower than those of wild-type virus in d106 and d109, respectively. In micrococcal-nuclease digestion experiments, nucleosomes were evident on the d109 genome, and the amount of total H3 as determined by chromatin immunoprecipitation was considerably greater on d109 than d106 genomes. The acetylation of histone H3 on the d106 genomes was evident at early and late times postinfection in Vero cells, but only at late times in HEL cells. The same pattern was observed for H3 acetylated on lysine 9. Trimethylation of H3K9 on d109 genomes was evident only at late times postinfection in Vero cells, while it was observed both early and late in HEL cells. Heterochromatin protein 1γ (HP1γ) was generally present only on d109 genomes at late times postinfection of HEL cells. The observations of chromatin structure correlate with the expression patterns of the three analyzed genes on the quiescent genomes. Therefore, several mechanisms generally affect the expression and contribute to the silencing of persisting genomes. These are the abundance of nucleosomes, the acetylation state of the histones, and heterochromatin. The extents to which these different mechanisms contribute to repression vary in different cell types and are counteracted by the presence of ICP0.

Early in productive infection, the herpes simplex type 1 (HSV-1) genome becomes bound with what appears to be an irregular arrangement of histones, and the presence of nucleosomes has not been established (20, 21, 24, 31, 39). In contrast, nucleosomes have been found associated with latent HSV-1 genomes (23), as well as, possibly, heterochromatin (8). During latency, there is little to no viral-gene expression, with the predominant expressed gene being that for the latency-associated transcript (54, 55). This suggests a general repression of transcription, probably as a result of epigenetic mechanisms. DNA methylation is probably not the major means of control of HSV-1 gene expression because latent HSV-1 DNA is not extensively methylated (5, 28). In contrast, a number of studies have implicated chromatin structure and specific histone tail modifications in the control of HSV-1 latency, reactivation, and replication (1, 7, 26, 30, 62, 64). Thus, histone association and chromatin structure during the early stages of infection are likely to be involved in determining the extent of viral-gene expression, and hence, whether productive or latent infection ensues (25).

Expression of ICP0 during this initial phase of infection may play a major role in determining which type of infection HSV-1 undergoes. ICP0 colocalizes with and causes the disruption of ND10 bodies, which are discrete multiprotein nuclear structures (4, 13, 17, 36). The RING finger ubiquitin ligase domain of ICP0 mediates the proteasomal degradation of the promyelocytic leukemia and Sp100 proteins, which are components of ND10 domains (17). The heterochromatin-binding protein HP1 interacts with Sp100 and can also be found at centromeres, forming a link between the disruption of ND10 bodies and chromatin (9). ICP0 also mediates the degradation of the centromere-associated proteins CENP-A (34) and CENP-C (10) in a proteasome-dependent manner. CENP-A is a histone H3-like centromere core protein thought to be involved in the assembly of heterochromatin (58). CENP-C also interacts with proapoptotic proteins, so degradation of CENP-C may be a viral mechanism to inhibit apoptosis, as well as to disrupt heterochromatin (44).

ICP0 also leads to the disruption of several transcriptionally repressive protein complexes. The C-terminal amino acids 537 to 613 of ICP0 share significant homology with a segment of CoREST (15). Histone deacetylases (HDACs) 1 and 2 form a complex with the REST and CoREST repressors of gene expression in nonneuronal cells. ICP0 binds the REST-CoREST-HDAC1/2 complex and causes the dissociation of HDAC1/2. CoREST and HDAC1/2 are then phosphorylated by HSV-1 proteins independently of ICP0 and translocated to the cytoplasm (15). This mechanism may provide for the specific derepression of certain cellular and viral genes. ICP0 also interacts with class II HDAC4, -5, and -7 (35). Class II HDACs are

* Corresponding author. Mailing address: E1257 Biomedical Science Tower, Department of Molecular Genetics and Biochemistry, University of Pittsburgh School of Medicine, Pittsburgh, PA 15261. Phone: (412) 648-9947. Fax: (412) 624-1401. E-mail: ndeluca@pitt.edu.

▽ Published ahead of print on 17 June 2009.

found in multiprotein complexes with transcriptional repressors (62). HDAC4, -5, and -7 are involved in developmental pathways in neurons, and it has been hypothesized that ICP0 inhibits their repressive activity in order to promote neuronal survival during productive infection (35). Additionally, herpesviral homologs of ICP0 interact with HDACs (65).

HDAC inhibitors have also been shown to reactivate gene expression from quiescent genomes (22, 59). Quiescent infections of standard tissue culture cells with HSV-1 can be established using mutants defective in multiple genes that activate HSV gene expression or affect host cell metabolism (11, 21, 38, 46, 47, 49, 50). Trichostatin A (TSA) can activate otherwise repressed expression from the human cytomegalovirus (HCMV) promoter on quiescent genomes similarly to ICP0 in Vero cells prior to 24 h postinfection (p.i.) (59). However, at 7 days p.i., reactivation induced by TSA is significantly decreased compared to ICP0-mediated reactivation. These effects were also seen in neuronal cultures, with support cells even more poorly reactivated than neurons (59). Importantly, TSA poorly activates gene expression from quiescent genomes in primary human fibroblasts, even when added at the time of infection (12), suggesting there are repressive functions other than histone deacetylation that ICP0 can abrogate. Additionally, this higher-order repression seems to be cell type dependent. Therefore, there may be multiple mechanisms by which ICP0 mediates the derepression of the viral genome.

Our laboratory has been examining the characteristics of two viral mutants, d109 and d106 (49), as a model for some of the events that occur very early in infection or during latency in vivo. d109 is a viral mutant defective for all five immediate-early (IE) genes. It expresses green fluorescent protein (GFP) under the control of the HCMV IE promoter and establishes a persistent quiescent infection in several cell types, including Vero and HEL cells and primary trigeminal neurons (49). It is nontoxic to these cells, and the viral genome persists in a quiescent state in the cells for prolonged periods. This is similar to other quiescent systems that are based on the inactivation of multiple viral activators (11, 21, 38, 46, 47, 49, 50). d109 can be reactivated from quiescence by supplying ICP0 in *trans*. d106 expresses ICP0 and the GFP transgene but none of the other IE proteins (49). We used this system to investigate the epigenetic state of quiescent viral genomes at three different loci as a function of time after infection, cell type, and the presence of ICP0. This was compared to the levels of expression of genes at these loci. Our results suggest that the expression of the loci is generally influenced by multiple levels of epigenetic regulation that also differ quantitatively in different cell types. The expression of ICP0 resulted in a reduction of the number of histones on the genome, as well as of the extent of modifications that promote higher-order chromatin structure.

MATERIALS AND METHODS

Cells and viruses. Experiments were performed using Vero (African green monkey kidney) cells or HEL (human embryonic lung) cells from the American Type Culture Collection (ATCC) propagated as they recommended. The viruses used in this study were wild-type (wt) HSV-1 (KOS), which was propagated on Vero cells, and the IE mutants d106 and d109 (49). d106 was propagated on E11 cells and d109 on F06 cells as previously described (49).

ChIP. Chromatin immunoprecipitation (ChIP) analysis was carried out as previously described (51) with a few modifications. Vero or HEL cells (5×10^6) were plated in 100-mm dishes and infected with either d109 or d106 at a multiplicity of infection (MOI) of 10 at 4°C for 1 h with rocking every 10 min. After adsorption, the inoculum was aspirated and 37°C 5% Dulbecco's modified Eagle's medium was added. This was considered 0 h p.i. At 4 and 24 h p.i., the cells were treated with 1% formaldehyde for 10 min at 37°C, washed three times with cold phosphate-buffered saline containing protease inhibitors (67 ng/ml aprotinin, 1 ng pepstatin, 0.16 mM TLCK [*N*α-*p*tosyl-L-lysine chloromethyl ketone], 1 mM phenylmethylsulfonyl fluoride). The cells were pelleted at 3,000 rpm for 10 min at 4°C, resuspended in cold PIPES [piperazine-*N*,*N*′-bis(2-ethanesulfonic acid] lysis buffer (100 μl per million cells) containing protease inhibitors (5 mM PIPES, 85 mM KCl, 0.5% NP-40, 4 μg/ml aprotinin, 2 μg/ml pepstatin, 0.15 mM TLCK, and 0.6 mM phenylmethylsulfonyl fluoride), and incubated on ice for 15 min. The antibodies used were anti-histone H3 (Abcam; ab1791), anti-acetyl histone H3 (Millipore; 06-599), anti-acetyl histone H3 lysine 9 (Millipore; 07-352), anti-trimethyl histone H3 lysine 9 (Millipore; 07-442), and anti-heterochromatin protein 1γ (Millipore; 05-690). A "no-antibody control" was included for each ChIP experiment. When calculating ChIP results after quantitative PCR (qPCR), the value for the no-antibody control was subtracted from the immunoprecipitation results before the percent input of immunoprecipitation was calculated. Therefore, any values reported indicate an increase over the baseline. The baseline, or no-antibody control, was always considerably less than the results for the specific immunoprecipitations. In addition, the analysis was also performed on mock-infected cells to control for possible external contamination. All other procedures were as described previously (52).

MN digestion. Vero or HEL cells (2×10^7) were infected at an MOI of 20 PFU/cell with d109 or d106. Nuclei were isolated at the indicated time points, divided into four aliquots, and digested with 20 units micrococcal nuclease (MN) for 2, 10, or 30 min. DNA was isolated by phenol chloroform extraction and ethanol precipitation and separated on a 2% agarose gel, transferred to a Nytran membrane, probed with ^{32}P-labeled nick-translated HSV bacterial artificial chromosome (BAC) DNA (obtained from David Leib, Washington University), and exposed to Hybond film.

RNA isolation and reverse transcription. RNA was isolated with the Ambion RNaqueous −4PCR kit, following the included protocol. Briefly, 5×10^6 Vero or 7.5×10^6 HEL cells in 100-mm plates were infected at an MOI of 10 with d109, d106, or KOS at room temperature. RNA was harvested at the indicated time points by adding 500 μl lysis buffer, provided in the kit. The cells were scraped and vortexed. An equal volume of 67% ethanol was added, and the mixture was added to a filter, which was centrifuged at 12,500 rpm at 4°C for 1 min. The bound RNA was washed with wash buffers 1 and 2/3. RNA was eluted with 60 μl 65°C elution solution. The RNA was treated with DNase I at 37°C for 30 min to degrade any residual DNA.

Reverse transcription was performed using the Ambion reverse transcription kit following the included instructions. Total RNA (2 μg) was reverse transcribed in a reaction volume of 20 μl containing RNase inhibitor, oligo(dT) primers, 1 μl Moloney murine leukemia virus reverse transcriptase (RT), and 2 μl 10× reaction buffer. The reaction tube was incubated at 85°C for 5 min to remove RNA secondary structure, and the reverse transcription reaction was carried out for 1 h at 44°C. After the reverse transcription reaction was complete, the reaction tube was incubated at 95°C for 10 min in order to inactivate the RT. Eight microliters of cDNA was diluted 1:6 by adding 40 μl DNase/RNase-free H_2O for use in qPCRs. Additionally, 1 μg RNA was diluted in a total of 60 μl DNase/RNase-free H_2O for use as a negative control in qPCRs.

Real-time PCR. Reactions for ChIP or cDNA quantification were performed in triplicate using 5 μl of DNA for each reaction as described previously (51), with a few modifications. Before the 96-well reaction plate was set up, a master mixture was made containing 0.625 μl of each primer (stock concentration, 1 mM), 12.5 μl Applied Biosystems SYBR green super mixture with 1.0 μM 6-carboxy-X-rhodamine (Bio-Rad), and 6.25 μl of water for a total of 20 μl for each reaction. The final reaction volume was 25 μl, including the DNA. The primers used for ChIP and cDNA quantification and their locations relative to the transcription start site of the gene to be analyzed are given in Table 1. d106 DNA was also included in each plate in a standard curve of 1:10 dilutions from 500,000 to 50 copies per well, which covers the threshold cycle values for the ChIP DNA samples tested. qPCR was run on an ABI 7900HT Fast Real Time machine. The conditions for the run were as follows: stage 1, 50°C for 2 min; stage 2, 95°C for 10 min; and stage 3, 40 cycle repeats of 95°C for 15 s and 60°C for 1 min. At the end of the run, a dissociation curve was completed to determine the purity of the amplified products. The results were analyzed using the SDS 2.3 software from Applied Biosystems.

TABLE 1. Primers used for RT-PCR

Primer	Sequence	Position relative to transcription start site
tkprom[a]	CAGCTGCTTCATCCCCGTGG AGATCTGCGGCACGCTGTTG	−200 to +56
tkds1[b]	ACCCGCTTAACAGCGTCAACA CCAAAGAGGTGCGGGAGTTT	+15 to +84
gCprom[a]	CGCCGGTGTGTGATGATTT TTTATACCCGGGCCCCAT	−84 to −26
gCds1[b]	GGGTCCGTCCCCCCCAAT CGTTAGGTTGGGGGCGCT	+627 to +735
HCMVprom[a]	CATCTACGTATTAGTCATCGCTATTAC TGGAAATCCCCGTGAGTCA	−249 to −156
GFPds1[b]	GTCGTGCTGCTTCATGTG AGTTCATCTGCACCACCG	+166 to +278

[a] Promoter sequence.
[b] Downstream in mRNA.

RESULTS

RNA expression from quiescent genomes. GFP is abundantly expressed from the HCMV promoter on the d106 genome, whereas GFP is abundantly expressed only in a subpopulation of d109-infected cells (49, 59). An aim of this study was to examine the effects of the epigenetic state on the expression of viral genes. Therefore, it was of interest to determine how the physical state of chromatin on the HCMV promoter correlates with the expression of GFP. It was also of interest to examine the expression of genes distant from the strong HCMV promoter to determine the generality the epigenetic mechanisms. With the exception of ICP6 in d106 (49), the HSV genes on the d109 and d106 genomes are poorly expressed due to the absence of ICP4. However, transcription of early and late genes in the absence of ICP4 is detectable (50, 64). This is a consequence of cellular transcription factors functioning in the absence of viral regulators. Real-time PCR was used to quantify the levels of GFP (HCMV promoter driven), tk (an early gene), and gC (a late gene) mRNAs in d109- and d106-infected Vero and HEL cells at 4 and 24 h p.i. The levels of these transcripts in wt-virus-infected cells at 2, 4, and 8 h p.i. were also quantified for comparison. The abundance of GFP mRNA detected in KOS-infected cells was less than 10^3 molecules/μg RNA, whereas it was as much as 2.3×10^9 molecules/μg of mRNA in d106-infected Vero cells (Fig. 1). Therefore, the numbers of mRNA molecules measured in this experiment differed by approximately 6.5 orders of magnitude.

The amounts of GFP mRNA in d106-infected Vero cells were 2.5- and 30-fold more abundant than in d109-infected cells at 4 and 24 h, respectively. These differences were 14- and 360-fold in HEL cells at 4 and 24 h, respectively. Therefore, GFP expression in d109-infected cells decreased with time and was lower in HEL cells than in Vero cells. This is indicative of repression in the absence of ICP0, which becomes more restrictive over time and is possibly more pronounced in HEL cells than in Vero cells. At 4 h p.i., the levels of tk and gC RNA in cells infected with d106 and d109 were approximately 10^2- to 10^3- and 10^3- to 10^4-fold lower than in wt-virus-infected cells, respectively. In addition, depending upon the cell type and time p.i., the numbers of tk and gC mRNAs present in d106- and d109-infected cells were approximately 10^3 to 10^4 times less than those of GFP mRNA. However, the same pattern of expression seen for GFP, as described above, was also seen for the tk and gC genes. Therefore, despite the large difference in expression between the activity of the HCMV IE promoter and those driving expression of tk and gC in d109- and d106-infected cells, similar mechanisms appear to affect the expression of all three genes.

Histone deposition on the viral genome as a function of cell type and ICP0. Following entry at the plasma membrane, the nucleocapsid is transported to the nucleus, where the genome is inserted. Histones can be found on the viral genome early after infection (24, 42), and quiescent genomes are associated with histone H3 through day 6 p.i. (7). HSV-1 gene products most likely affect histone deposition on the genome. Both VP16 and VP22 have been reported to decrease histone deposition on the viral genome (20, 61). The activities of ICP0 are also consistent with effects on chromatin structure (10, 15, 16, 18, 34, 35, 45, 59). As a first step toward determining the epigenetic mechanisms that contribute to the expression profile shown in Fig. 1, two approaches were employed. The first examined the nucleosomal structure of the viral genome by MN analysis of nuclear DNA. The second was to quantify the total amount of histone H3 on the viral genomes.

Vero and HEL cells were infected with d109 and d106. At 4 and 24 h p.i, nuclei were prepared and subjected to MN analysis. The nuclei were incubated with MN for increasing lengths of time. The DNA was then isolated, run on an agarose gel, blotted onto nylon, and probed with ^{32}P-labeled HSV sequences. Figure 2 shows both the ethidium bromide (EtBr)-stained gel prior to blotting and the autoradiographic images of the exposed probed blot. The nucleosomal banding pattern of the bulk cellular DNA is clearly evident in the EtBr-stained gels of both cell types. The Southern blot was probed with purified ^{32}P-labeled HSV DNA contained in a BAC. Therefore, the observed pattern represents the sum of possible different patterns from different regions of the genome. However, a similar pattern was seen when the HCMV IE promoter was used as a probe (unpublished observations). A reproducible nucleosomal hybridization pattern was evident, particularly in d109-infected HEL cells (Fig. 2A); however, the pattern was more heterogeneous than the EtBr pattern observed for the bulk cellular DNA. Therefore, the chromatin on the d109 genome in HEL cells may be more organized. However, there are portions or populations of d109 genomes in HEL and Vero cells that result in a heterogeneous MN pattern. Nucleosomal structure was not reproducibly observed on d106 genomes in HEL or Vero cells. The observed heterogeneous pattern might have been due to less ordered nucleosomal structure, or despite the fact that only nuclei were subjected to the analysis, some of the genomes might still have been in capsids bound to the nuclei. None of the observed hybridization pattern was due to cross-hybridization to the cellular DNA, since mock-infected cell lanes were clear.

Another approach to probe the possible association of nucleosomes with the genomes is to determine the amount of bulk histone, in this case H3, by ChIP analysis. Vero and HEL cells were infected with d109 or d106 and at 4 and 24 h p.i. were subjected to ChIP analysis using an antibody against H3 (Fig. 3). The extent of sequences in the immunoprecipitate was determined by real-time PCR. In HEL cells (Fig. 3B), association of histone H3 with all three promoters on d109 could be

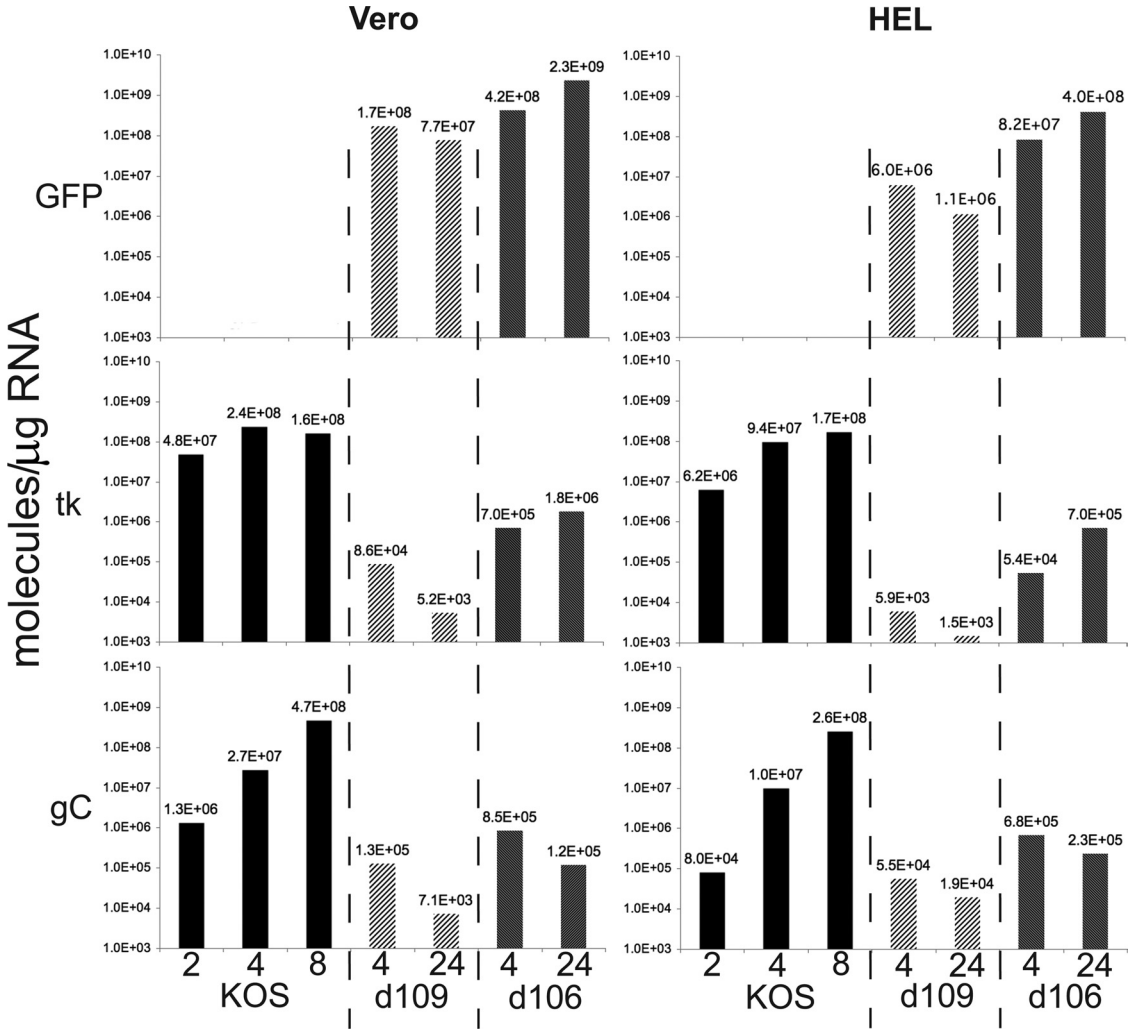

FIG. 1. Abundances of GFP, tk, and gC mRNAs in KOS-, d109-, and d106-infected Vero and HEL cells. Infections, RNA isolation, cDNA preparation, and RT-PCR with primer sets for the indicated mRNAs were performed as described in Materials and Methods. The procedure for creating standard curves for quantification using the indicated primers is also described in Materials and Methods. The graphs indicate the number of RNA molecules of each gene per μg RNA at the indicated time points (2, 4, 8, and 24 h p.i.) in Vero and HEL cells.

seen at 4 h p.i., and it had increased by 24 h p.i. In contrast, the association of histone H3 with d106 was greatly reduced and never rose above a low level. A similar pattern of histone association occurred in Vero cells, except that the histone H3 association with the tk promoter of d109 only marginally increased from 4 to 24 h p.i.

The results of the ChIP (Fig. 3) and the MN (Fig. 2) assays are consistent in that they suggest greater nucleosomal association with the d109 than the d106 genome. The increase in H3 on the d109 genome (Fig. 3) is also consistent with the decreased expression from the d109 genome at 24 p.i. (Fig. 1). The reduced amounts of H3 on the viral genome during d106 infection are consistent with the greater expression of the d106 genome (Fig. 1) and are possibly indicative of interference in histone deposition by ICP0.

Acetylation of histone H3 on quiescent viral genomes is a function of ICP0. Histone H3 hyperacetylation (AcH3) is associated with increased transcriptional activity (52). Lytic infection has been shown to increase global cellular levels of acetylated histone H3 (24), and ICP0 has been implicated in increasing the acetylation of histones on the viral genome (6, 7). ICP0 has also been shown to inhibit repressive complexes that include HDAC inhibitors (15, 16). Additionally, HDAC inhibitors, such as TSA, have been shown to increase HSV-1 expression and to derepress HSV quiescence in a manner similar to that of ICP0 in Vero cells (22, 59).

ChIP was used to determine the extent of AcH3 on the d109 and d106 genomes in Vero and HEL cells. In Vero cells, AcH3 was low on all the promoters on the d109 genomes but was elevated on d106 genomes at both 4 and 24 h p.i. (Fig. 4A). The extent of H3 acetylation in d106-infected cells is masked by the fact that there is less total H3 on the genomes. This is clearly seen when the amount of AcH3 is divided by the total H3 (Fig. 4C). Therefore, while the amount of AcH3 on the HCMV promoter is not much greater than that in d109-infected cells, the H3 that is on the d106 genomes is more extensively acetylated. The same general pattern was observed in HEL cells (Fig. 4B and D), although the amounts and

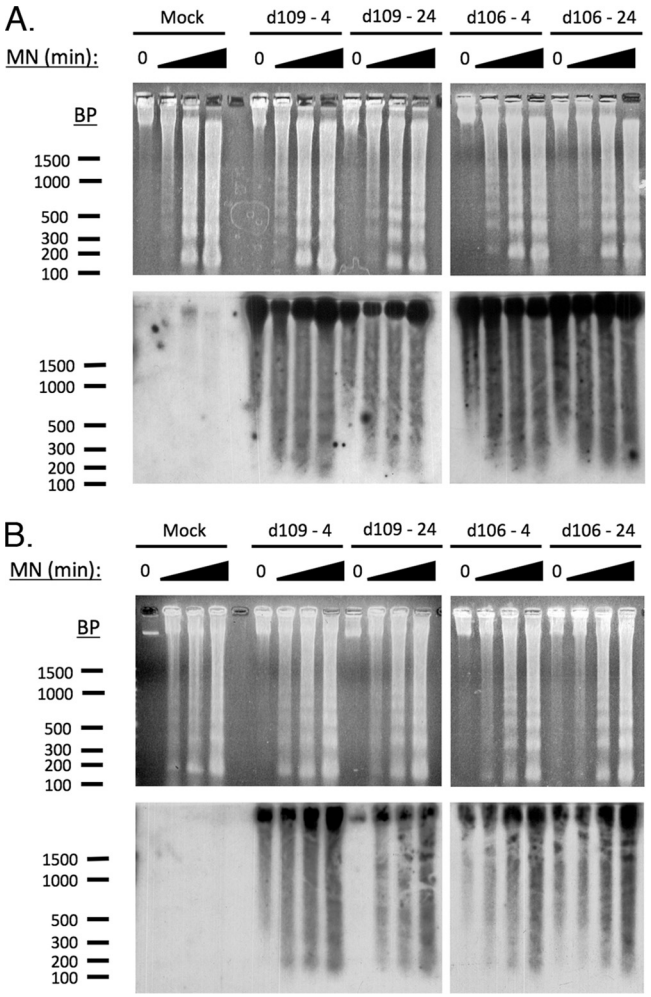

FIG. 2. MN digestion of d109- and d106-infected cells. Nuclei were isolated from d109-, d106-, or mock-infected HEL cells (A) or Vero cells (B) and digested with 20 units MN for 2, 10, or 30 min. The DNA was isolated from the nuclei at 4 and 24 h p.i., purified, and fractionated on 2.0% agarose gels. The agarose gels were stained with EtBr (top) and transferred to Nytran membranes for Southern blot hybridization as described in Materials and Methods. The Southern blots (bottom) were probed with ^{32}P-labeled HSV BAC DNA, washed, and exposed to X-ray film. Shown are the autoradiographic images of the probed blots (bottom).

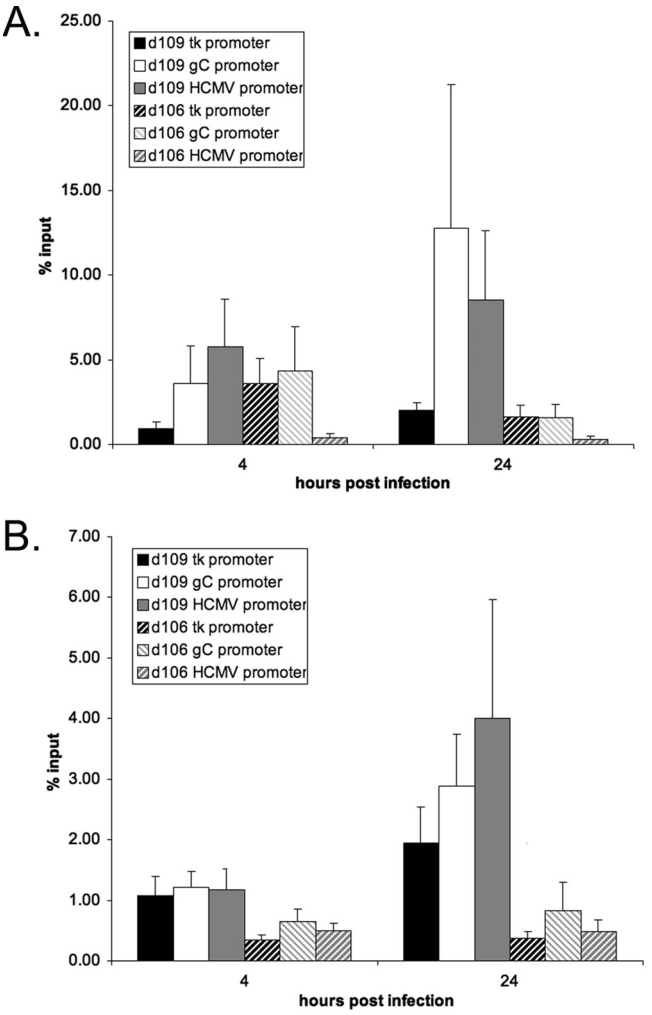

FIG. 3. Binding of histone H3 to the tk, gC, and HCMV promoters of d109 and d106 in Vero and HEL cells. ChIP with an antibody to histone H3 and RT-PCR with primer pairs corresponding to the indicated promoter regions were performed as described in Materials and Methods. The graphs show the percentages of total genomes bound at 4 and 24 h p.i. in Vero cells (A) and HEL cells (B). The error bars represent standard deviations from multiple experiments.

fraction of AcH3 on the promoters in d106-infected cells were not as elevated relative to d109 as in Vero cells. This is consistent with the lower level of expression in HEL cells.

To further investigate the effects of the cell type and ICP0 on the acetylation state of histones associated with quiescent genomes, we performed ChIP for acetylated histone H3 lysine 9 (H3AcK9) (Fig. 5). This specific modification has been associated with increased transcription. This may be due to the loss of the positive charge of lysine and decreased electrostatic attraction of the histone tail to the DNA backbone, and/or it may increase transcription by preventing histone H3 lysine 9 methylation (H3meK9), which is associated with a decrease in the rate of transcription.

The amounts of H3AcK9 on the promoters in d109-infected cells were relatively low (Fig. 5A and B). Also, as shown in Fig. 4, the exception is the HCMV promoter at 4 h p.i., where the amount of H3AcK9 was elevated relative to the other promoters in both cell types. The amount of H3AcK9 on the d106 genome was readily evident at 4 h p.i. in Vero cells (Fig. 5A and C), whereas it was not in HEL cells but became detectable later in infection (Fig. 5B and D). Therefore, the pattern of H3AcK9 was similar to that of AcH3 on the tk, gC, and HCMV promoters of d109 and d106 in both Vero and HEL cells.

Effects of cell type and ICP0 on repressive chromatin structure. The global repression of HSV during latency is likely due to epigenetic mechanisms. Histone lysine methylation is associated with both activation and repression of transcription, depending on which residue is modified (3, 26). These modifications may recruit additional proteins that help to either silence or activate transcription. Trimethylation of histone H3 lysine 9 (H3me3K9) is correlated with repression of expression (3). Lysine methylation does not remove a positive charge from

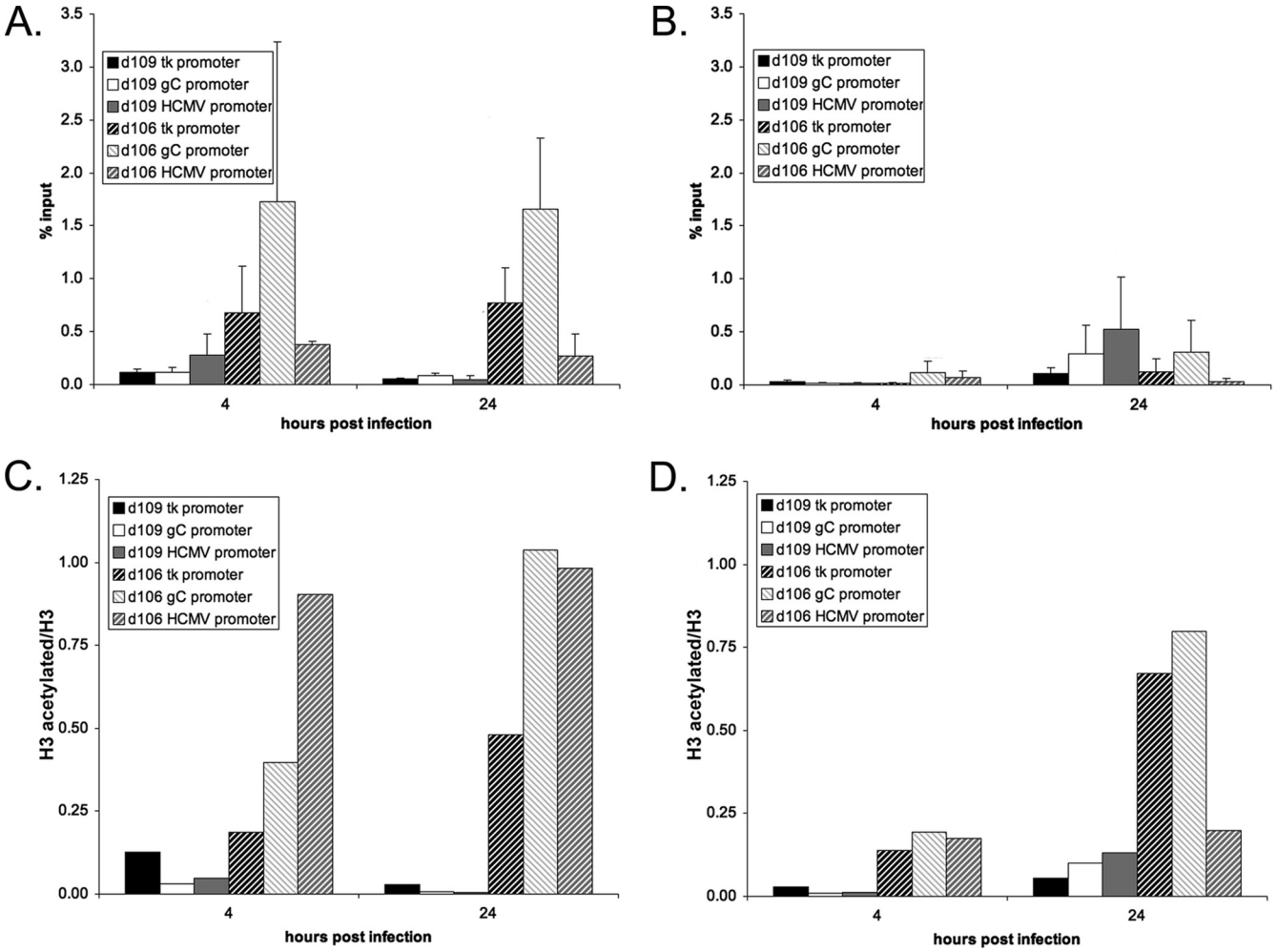

FIG. 4. Binding of AcH3 to the tk, gC, and HCMV promoters of d109 and d106 in Vero and HEL cells. ChIP with an antibody to AcH3 and RT-PCR were performed as described in the legend to Fig. 3 to determine the percentages of genomes bound by AcH3 at 4 and 24 h p.i. in Vero (A) and HEL (B) cells. The error bars represent standard deviations from multiple experiments. In order to compensate for the reduced histone H3 on d106 promoters, AcH3 was normalized to the amount of histone H3 on the genome by dividing the percentage of AcH3 associated with each promoter by the percent histone H3 (Fig. 3) in Vero cells (C) and HEL cells (D).

the histone tail and also precludes acetylation. Additionally, histone lysine methylation is a very stable histone modification (48), which could help to form the basis of long-term quiescence. H3me3K9 is a binding site for heterochromatin protein 1 (HP1) (2, 29, 40), which helps to silence transcription and to form higher-order chromatin structure (30, 33).

We investigated the presence of H3me3K9 and HP1γ by ChIP analysis (Fig. 6). H3me3K9 was rarely found on the d109 genomes in Vero cells at 4 h p.i. or on the d106 genomes in both HEL and Vero cells (Fig. 6A and B). In HEL cells, H3me3K9 was detected on all three promoters on the d109 genome at both 4 and 24 h p.i. (Fig. 6B). However, H3me3K9 was detected on the gC and HCMV IE promoters only on the d109 genome in Vero cells at 24 h p.i. (Fig. 6A). HP1γ helps to form higher-order chromatin structure and binds to H3me3K9. The amounts of HP1γ binding to the HCMV, tk, and gC promoters of d109- and d106-infected HEL and Vero cells were determined by ChIP. HP1γ was rarely found on the d109 genomes at 4 h p.i. or on the d106 genome under any circumstances (Fig. 6C and D). In d109-infected Vero cells, HP1γ was seen only on the gC promoter at 24 h (Fig. 6C), whereas it was detected on all three of the promoters in d109-infected HEL cells at 24 h (Fig. 6D).

Considering d109 infection, the general pattern that arises from the data in Fig. 6 is that (i) H3 methylation precedes HP1γ association, (ii) H3 methylation occurs more rapidly in HEL cells than in Vero cells, and (iii) HP1γ association is only generally seen at 24 h p.i. of HEL cells. These data are consistent with a more restrictive environment for gene expression from the d109 genome in HEL than in Vero cells (Fig. 1). Reduced amounts of H3 methylation and HP1γ deposition were consistently observed in d106-infected cells, suggesting a direct or indirect inhibitory effect of ICP0 on this repressive mechanism.

DISCUSSION

The mutant virus d109 does not express HSV IE proteins and is subject to repression, where even the relatively potent

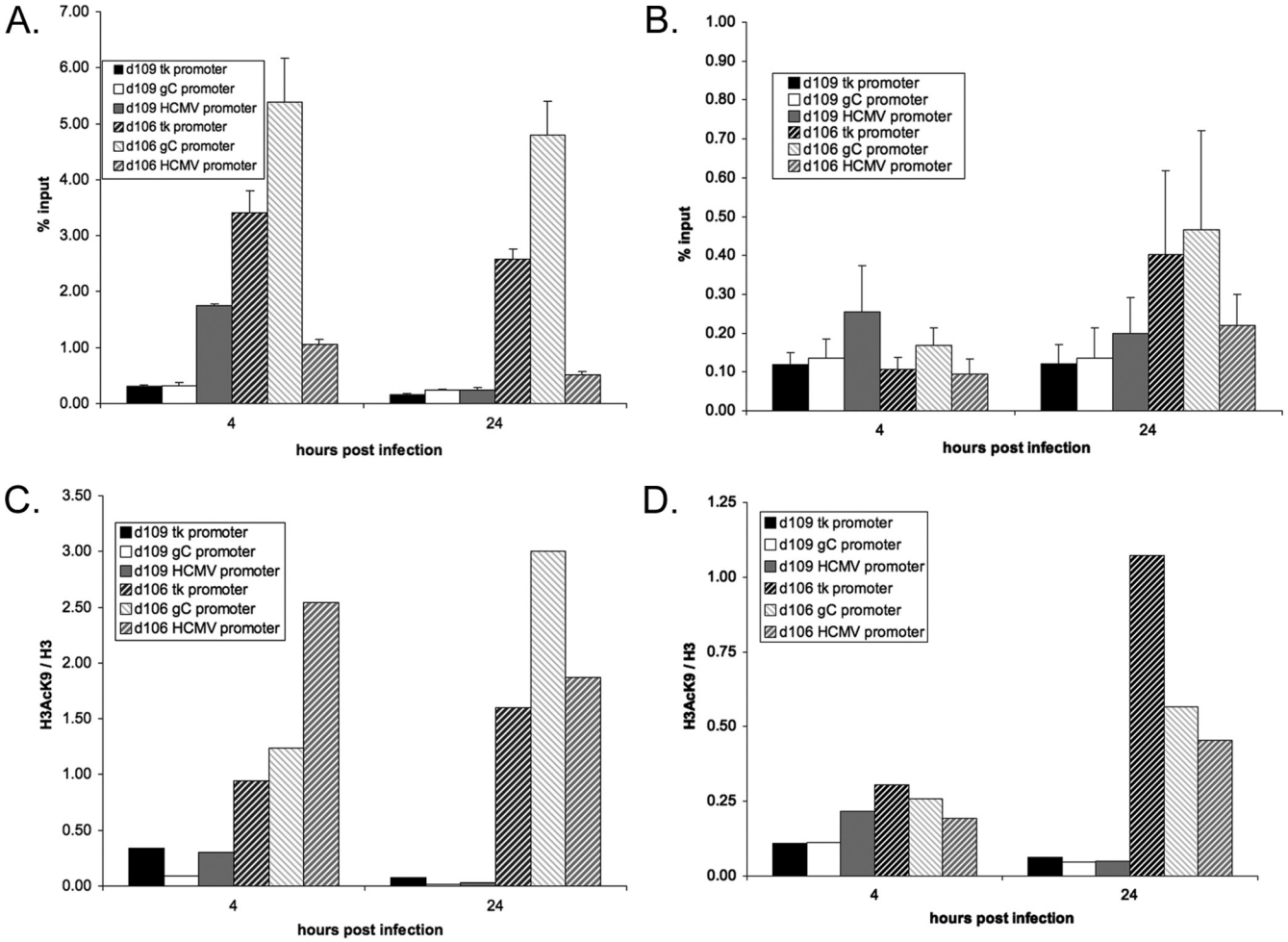

FIG. 5. Binding of H3AcK9 to the tk, gC, and HCMV promoters of d109 and d106 in Vero and HEL cells. ChIP with an antibody to H3AcK9 and RT-PCR were performed as described in the legend to Fig. 3 to determine the percentage of genomes bound by H3AcK9 at 4 and 24 h p.i. in Vero (A) and HEL (B) cells. The error bars represent standard deviations from multiple experiments. In order to compensate for the reduced histone H3 on d106 promoters, AcH3 was normalized to the amount of histone H3 on the genome by dividing the percentage of AcH3 associated with each promoter by the percent histone H3 (Fig. 3) in Vero cells (C) and HEL cells (D).

HCMV IE promoter is abundantly expressed only in a subpopulation of infected cells. d109 genomes persist in a quiescent state in most cell types. Thus, aspects of the cellular mechanisms influencing quiescent genomes in culture may reflect HSV latency. Both nucleosomes and heterochromatin have been associated with HSV latency in animal models (8, 63). In this study, ChIP was used to examine the states of chromatinization of three promoters with different relative activities and locations on quiescent viral genomes and to observe how this state may be affected by the expression of ICP0 and possibly differ in different cell types. We examined the deposition of nucleosomes on the genomes and focused on histone H3 with respect to its abundance on the genomes, acetylation (total and lysine 9) and methylation (lysine 9) states, and the presence of the hetrochromatin protein HP1γ. The chromatinization state was correlated with the levels of expression at the three analyzed loci.

Gene expression as a function of IE proteins. In the absence of the IE proteins ICP4, -27, and -22 (d106-infected cells), expression levels of the tk and gC loci were dramatically reduced relative to that seen in KOS-infected cells (Fig. 1), largely due to the absence of ICP4, which is the major activator of early and late genes. Unlike tk and gC, expression from the HCMV IE promoter was abundant in d106-infected cells. This is presumably due to the presence of the strong enhancer in the HCMV IE promoter (56, 57, 60). The additional lack of ICP0 expression (d109) further lowered the expression of the HCMV IE, tk, and gC promoters. This was more pronounced at 24 h than at 4 h p.i., suggesting either an activation of expression in the presence of ICP0 or the active inhibition of transcription in the absence of ICP0. Expression was generally lower in HEL cells than in Vero cells. In addition, the difference in expression in the presence of ICP0 relative to expression in its absence was greater in HEL cells than in Vero cells. This is consistent with a greater involvement of repression mechanisms functioning on the genome in HEL cells.

Deposition of nucleosomes and histone H3 as a function of ICP0. Nucleosomal structure as visualized by MN analysis was evident on d109 genomes, particularly in HEL cells (Fig. 2). It was less evident for d106 genomes. However, in both d106 and

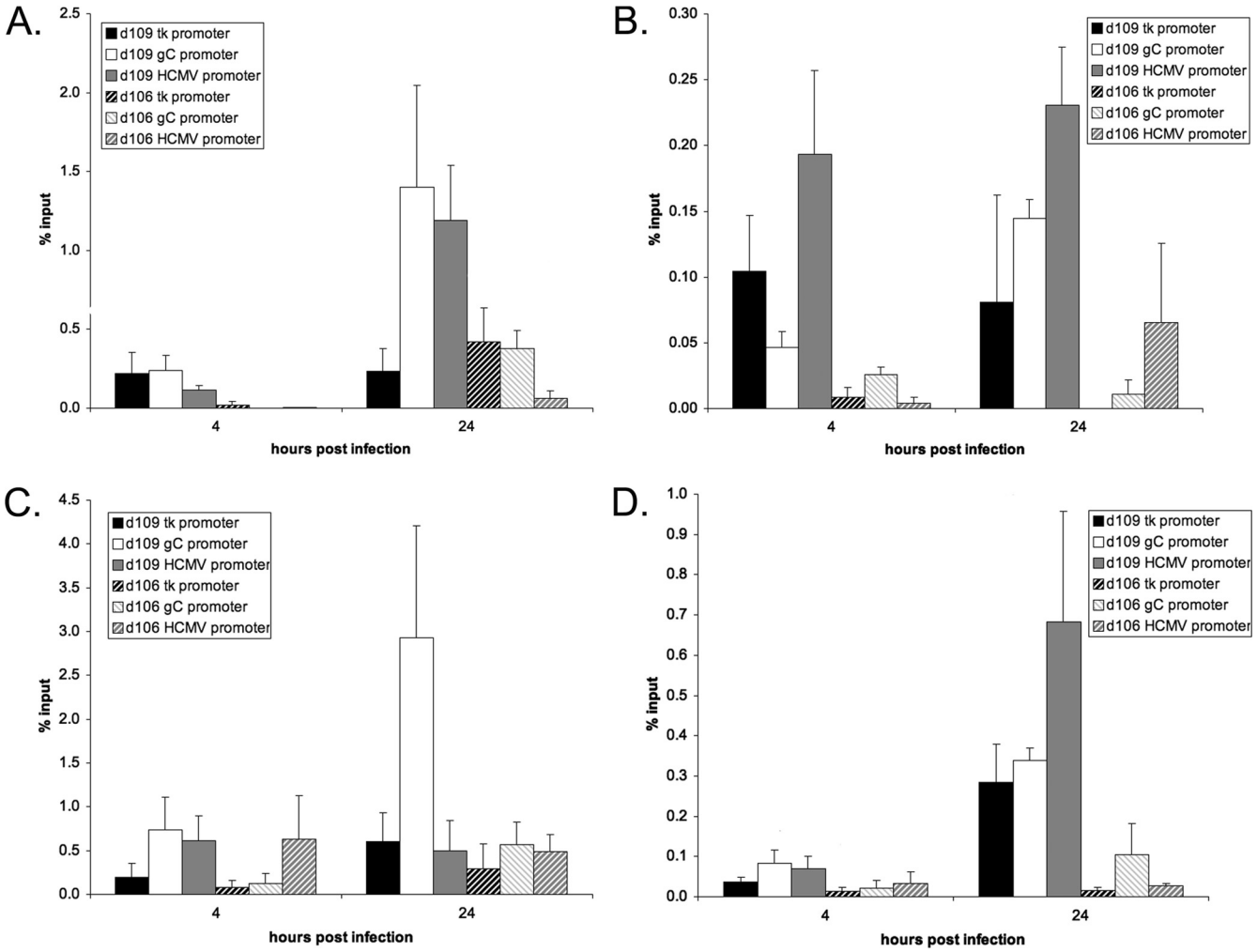

FIG. 6. Repressive chromatin modifications associated with the tk, gC, and HCMV promoters of d109 and d106 in Vero and HEL cells. ChIP with antibodies to H3me3K9 (A and B) and HP1γ (C and D), followed by RT-PCR, was performed as described in the legend to Fig. 3 to determine the percentages of genomes bound by H3me3K9 (A and B) and HP1γ (C and D) at 4 and 24 h p.i. in Vero (A and C) and HEL (B and D) cells. The error bars represent standard deviations from multiple experiments.

d109, there was a background of nuclease digestion products that was not consistent with an ordered nucleosomal structure. Previous studies of wt HSV suggested that during productive infection there is little nucleosomal structure and that the genome may be more sensitive to MN digestion (31, 32). The more heterogeneous component in the MN analysis in our studies may be similar to that observed in these previous studies. However it is not entirely appropriate to compare wt infections to those analyzed in this study. Unlike that of wt virus, the genomes of d106 and d109 are not replicating and are not being packaged. In wt virus infections, these processes typically begin at 4 and 6 h, respectively, and undoubtedly influence the MN analysis. A more appropriate comparison is a previous study by Jamieson et al. (23), which did not find an ordered nucleosomal structure on the tk promoter in cells infected with a mutant defective in VP16 and with restricted expression of ICP0 in the presence of alpha interferon. The difference between our results and these may be the extent of IE gene inactivation in the two systems. Alternatively, there may be little difference at all. In both studies, the analysis was complicated by the fact that not all infecting genomes are exposed to the cellular machinery in the nucleus. The previous study hypothesized that many of the genomes did not uncoat, for example. In addition, while the entire HSV-1 genome was used as a probe in Fig. 2, the use of promoter-specific probes revealed little difference from the results in Fig. 2 (unpublished observations).

As an alternative approach to examining possible nucleosomal deposition on quiescent genomes, the abundance of bulk histone H3 was determined by ChIP analysis (Fig. 3). The expression of ICP0 resulted in decreased association of H3 at all three promoter loci in both HEL and Vero cells (Fig. 3). Therefore, the presence of ICP0 somehow prevents the association of histone H3 with the genome. The reduced association of H3 in the presence of ICP0 is probably not a function of transcription, since the amounts of H3 on the tk and gC promoters are comparable to that on the HCMV IE promoter in d106-infected HEL cells, despite the observation that the tk

and gC promoters are 2 to 3 orders of magnitude less transcriptionally active than the HCMV IE promoters (Fig. 1).

A recent study by Coleman et al. (7) investigated H3 association with quiescent genomes upon reactivation from quiescence and found that although hyperacetylation of the histones bound to the viral genome occurred upon the expression of ICP0, the total amount of bound histone H3 remained constant upon reactivation. This indicates that ICP0 does not facilitate the removal of histones from the viral genome. Our study, in which ICP0 is expressed from the outset of infection, suggests that it is able to prevent the deposition of histone H3 onto all three types of viral promoters. This is consistent with a study showing that ICP0 prevented the binding of H3 to the genome during productive infection (6). This may occur by relocalization or degradation of histones or histone chaperones, which subsequently leads to a more open viral-genome configuration in which the availability of transcription factors can control expression unimpeded by epigenetic structure.

ICP0 causes increased acetylation of histone H3 bound to the viral genome (7). ICP0 interacts with and causes the relocalization of class II HDACs (35). It is also known to disrupt the REST-CoREST-HDAC complex (15, 16), which is able to inhibit ICP4 expression in transient-transfection assays (43). This inhibition is counteracted by the addition of TSA, an HDAC inhibitor. TSA can also partially substitute for ICP0 in the reactivation of gene expression from quiescent HSV genomes (59), and the effects of d106 on cellular-gene expression are similar to those induced by the addition of TSA (22). In our study, it was difficult to assess the hyperacetylation of histone H3 on the viral promoters simply by quantifying the abundance of AcH3. The total amount of hyperacetylated histone H3 associated with the viral promoters was not uniformly increased in d106 infection over that in d109 infection (Fig. 4). This was most pronounced in HEL cells (Fig. 4B) and is because the amount of total H3 on the genome is greatly reduced (Fig. 3). When the amount of AcH3 was normalized to the total amount of H3, there was a significant increase in acetylation of the histones associated with d106. Thus, the small number of histones that become associated with the viral genome are generally found in an acetylated state. The histones bound to the d106 HCMV, tk, and gC promoters are hyperacetylated in comparison to those on the d109 viral promoters in both HEL and Vero cells (Fig. 4). This is consistent with the 1- to 3-order-of-magnitude increase in gene expression from d106 relative to d109. This hyperacetylation of histone H3 may be due to ICP0-mediated reduction of HDAC activity. A number of studies have suggested that this is mechanistically connected to the disruption of ND10 through the ubiquitin ligase activity of ICP0 and/or the ability of ICP0 to disrupt REST-coREST/HDAC complexes (15, 16–19).

ICP0 expression also resulted in the specific hyperacetylation of histone H3 lysine 9 (Fig. 5). Although histone acetyltransferase (HAT) activity is somewhat generalized, specific residues of histone tails are generally acetylated by specific HATs. H3K9 acetylation has been linked to the HATs GCN5 and PCAF (14, 27). ICP0 may increase the activities of these HATs, as well as others. ICP0 colocalizes with the HATs CBP and p300 and can be coimmunoprecipitated with p300 (37). Thus, ICP0 may have an effect on HAT activity, concurrent with its decrease of HDAC activity, leading to the hyperacetylation of histones bound to the viral genome and a subsequent increase in transcription.

AcH3 and H3AcK9 were observed on the d106 genome at 4 h p.i. in Vero cells (Fig. 4A and C and 5A and C). They were not observed on the d106 genome in HEL cells at that time (Fig. 4B and D and 5B and D). This may be because positive effects of ICP0 competed with the cellular repression mechanisms, which may be more potent in HEL than in Vero cells. The repression of viral genomes is considered below.

Formation of repressive chromatin. H3me3K9 occurs exclusively of H3AcK9 and vice versa. It is a binding site for HP1γ, which is a component of heterochromatin, a repressive chromatin structure. H3me3K9 was seen very early in the infection of HEL cells (Fig. 6B), whereas it was detected only at the 24-h point in Vero cells (Fig. 6B). The formation of heterochromatin, as seen by the binding of HP1γ, occurs only after the trimethylation of histone H3. This is consistent with the observation that HP1γ binding follows H3me3K9 presence on the d109 genomes in HEL cells (Fig. 6B and D). HP1γ was detected in Vero cells only on the gC promoter in the d109 genome at 24 h p.i. Interestingly, gC is the only gene expressed by d109 at a higher level in HEL cells than in Vero cells at 24 h p.i. This exception aside, the lack of heterochromatin formation in Vero cells is consistent with the greater transcriptional activity of the d109 genome in Vero cells than in HEL cells. This observation also explains the greater ease with which expression can be reactivated with HDAC inhibitors, such as TSA, from quiescent genomes in Vero cells as opposed to HEL cells.

Heterochromatin formation appears to be a process that is inhibited by ICP0. ICP0 may actively prevent the methylation of histones by inhibiting the activity of a histone methyltransferase or increasing the activity of a histone demethylase. However, it is more likely that the decreased H3me3K9 and HP1γ binding on the d106 genome is a downstream effect due to the decrease in H3 binding and an increase in H3K9 acetylation, with the latter precluding K9 methylation. This would not explain the reported decrease in H3meK9 following reactivation with ICP0 without a decrease in H3 binding (7). This is remarkable, considering that methylation of histones is considered a long-lived modification (48), which until recently was thought to remain until the histone is replaced or the tail removed (53). It is possible that the reversal of heterochromatin formation upon ICP0-mediated reactivation may be different from the mechanism by which it prevents heterochromatin formation.

The results of these studies indicate that a complex, multistep process occurs in the formation of a silenced and heterochromatic state of the HSV genome. Multiple levels of chromatin structure can be observed in the quiescent genome system, and these levels of chromatin structure correlate with gene expression levels. The observations that we made under any given condition probably represent the sum of a number of chromatin states. A subpopulation of d109-infected Vero (~10%) and HEL (~0.1%) cells abundantly express GFP from the HCMV IE promoter (59), indicative of multiple populations of genome states. Heterochromatin has been observed in latently infected mouse ganglia (63). However, it is possible that the multiple states of repression observed in this study exist in latency, as well. Primary trigeminal neurons are more

permissive for gene expression from the d109 genome than support cells (59). Moreover, quiescent genomes in primary neurons are more readily activated by TSA (1, 59). Reactivation of latently infected ganglia by the HDAC inhibitor sodium butyrate has also been observed (41). These observations suggest that genomes persisting in latency are not necessarily repressed by heterochromatin. The more relaxed repression may allow for more readily reactivated genomes, leading to some viral-gene expression, which could lead to abortive or productive reactivation events.

ACKNOWLEDGMENTS

This work was supported by NIH grant R01 AI044821 to N.A.D. M.W.F. is funded by training grant T32 AI049820.

REFERENCES

1. **Arthur, J. L., C. G. Scarpini, V. Connor, R. H. Lachmann, A. M. Tolkovsky, and S. Efstathiou.** 2001. Herpes simplex virus type 1 promoter activity during latency establishment, maintenance, and reactivation in primary dorsal root neurons in vitro. J. Virol. **75:**3885–3895.
2. **Bannister, A. J., P. Zegerman, J. F. Partridge, E. A. Miska, J. O. Thomas, R. C. Allshire, and T. Kouzarides.** 2001. Selective recognition of methylated lysine 9 on histone H3 by the HP1 chromo domain. Nature **410:**120–124.
3. **Barski, A., S. Cuddapah, K. Cui, T. Y. Roh, D. E. Schones, Z. Wang, G. Wei, I. Chepelev, and K. Zhao.** 2007. High-resolution profiling of histone methylations in the human genome. Cell **129:**823–837.
4. **Boutell, C., A. Orr, and R. D. Everett.** 2003. PML residue lysine 160 is required for the degradation of PML induced by herpes simplex virus type 1 regulatory protein ICP0. J. Virol. **77:**8686–8694.
5. **Buschhausen, G., M. Graessmann, and A. Graessmann.** 1985. Inhibition of herpes simplex thymidine kinase gene expression by DNA methylation is an indirect effect. Nucleic Acids Res. **13:**5503–5513.
6. **Cliffe, A. R., and D. M. Knipe.** 2008. Herpes simplex virus ICP0 promotes both histone removal and acetylation on viral DNA during lytic infection. J. Virol. **82:**12030–12038.
7. **Coleman, H. M., V. Connor, Z. S. Cheng, F. Grey, C. M. Preston, and S. Efstathiou.** 2008. Histone modifications associated with herpes simplex virus type 1 genomes during quiescence and following ICP0-mediated de-repression. J. Gen. Virol. **89:**68–77.
8. **Deshmane, S. L., and N. W. Fraser.** 1989. During latency, herpes simplex virus type 1 DNA is associated with nucleosomes in a chromatin structure. J. Virol. **63:**943–947.
9. **Everett, R. D.** 2000. ICP0, a regulator of herpes simplex virus during lytic and latent infection. Bioessays **22:**761–770.
10. **Everett, R. D., W. C. Earnshaw, J. Findlay, and P. Lomonte.** 1999. Specific destruction of kinetochore protein CENP-C and disruption of cell division by herpes simplex virus immediate-early protein Vmw110. EMBO J. **18:**1526–1538.
11. **Everett, R. D., J. Murray, A. Orr, and C. M. Preston.** 2007. Herpes simplex virus type 1 genomes are associated with ND10 nuclear substructures in quiescently infected human fibroblasts. J. Virol. **81:**10991–11004.
12. **Everett, R. D., C. Parada, P. Gripon, H. Sirma, and A. Orr.** 2008. Replication of ICP0-null mutant herpes simplex virus type 1 is restricted by both PML and Sp100. J. Virol. **82:**2661–2672.
13. **Everett, R. D., and A. Zafiropoulos.** 2004. Visualization by live-cell microscopy of disruption of ND10 during herpes simplex virus type 1 infection. J. Virol. **78:**11411–11415.
14. **Grant, P. A., A. Eberharter, S. John, R. G. Cook, B. M. Turner, and J. L. Workman.** 1999. Expanded lysine acetylation specificity of Gcn5 in native complexes. J. Biol. Chem. **274:**5895–5900.
15. **Gu, H., Y. Liang, G. Mandel, and B. Roizman.** 2005. Components of the REST/CoREST/histone deacetylase repressor complex are disrupted, modified, and translocated in HSV-1-infected cells. Proc. Natl. Acad. Sci. USA **102:**7571–7576.
16. **Gu, H., and B. Roizman.** 2007. Herpes simplex virus-infected cell protein 0 blocks the silencing of viral DNA by dissociating histone deacetylases from the CoREST REST complex. Proc. Natl. Acad. Sci. USA **104:**17134–17139.
17. **Gu, H., and B. Roizman.** 2003. The degradation of promyelocytic leukemia and Sp100 proteins by herpes simplex virus 1 is mediated by the ubiquitin-conjugating enzyme UbcH5a. Proc. Natl. Acad. Sci. USA **100:**8963–8968.
18. **Gu, H., and B. Roizman.** 2009. Engagement of the lysine-specific demethylase/HDAC1/CoREST/REST complex by herpes simplex virus 1. J. Virol. **83:**4376–4385.
19. **Gu, H., and B. Roizman.** 2009. The two functions of herpes simplex virus 1 ICP0, inhibition of silencing by the CoREST/REST/HDAC complex and degradation of PML, are executed in tandem. J. Virol. **83:**181–187.
20. **Herrera, F. J., and S. J. Triezenberg.** 2004. VP16-dependent association of chromatin-modifying coactivators and underrepresentation of histones at immediate-early gene promoters during herpes simplex virus infection. J. Virol. **78:**9689–9696.
21. **Hobbs, W. E., D. E. Brough, I. Kovesdi, and N. A. DeLuca.** 2001. Efficient activation of viral genomes by levels of herpes simplex virus ICP0 insufficient to affect cellular gene expression or cell survival. J. Virol. **75:**3391–3403.
22. **Hobbs, W. E., and N. A. DeLuca.** 1999. Perturbation of cell cycle progression and cellular gene expression as a function of herpes simplex virus ICP0. J. Virol. **73:**8245–8255.
23. **Jamieson, D. R., L. H. Robinson, J. I. Daksis, M. J. Nicholl, and C. M. Preston.** 1995. Quiescent viral genomes in human fibroblasts after infection with herpes simplex virus type 1 Vmw65 mutants. J. Gen. Virol. **76:**1417–1431.
24. **Kent, J. R., P. Y. Zeng, D. Atanasiu, J. Gardner, N. W. Fraser, and S. L. Berger.** 2004. During lytic infection herpes simplex virus type 1 is associated with histones bearing modifications that correlate with active transcription. J. Virol. **78:**10178–10186.
25. **Knipe, D. M., and A. Cliffe.** 2008. Chromatin control of herpes simplex virus lytic and latent infection. Nat. Rev. Microbiol. **6:**211–221.
26. **Koch, C. M., R. M. Andrews, P. Flicek, S. C. Dillon, U. Karaoz, G. K. Clelland, S. Wilcox, D. M. Beare, J. C. Fowler, P. Couttet, K. D. James, G. C. Lefebvre, A. W. Bruce, O. M. Dovey, P. D. Ellis, P. Dhami, C. F. Langford, Z. Weng, E. Birney, N. P. Carter, D. Vetrie, and I. Dunham.** 2007. The landscape of histone modifications across 1% of the human genome in five human cell lines. Genome Res. **17:**691–707.
27. **Kouzarides, T.** 2007. Chromatin modifications and their function. Cell **128:**693–705.
28. **Kubat, N. J., R. K. Tran, P. McAnany, and D. C. Bloom.** 2004. Specific histone tail modification and not DNA methylation is a determinant of herpes simplex virus type 1 latent gene expression. J. Virol. **78:**1139–1149.
29. **Lachner, M., D. O'Carroll, S. Rea, K. Mechtler, and T. Jenuwein.** 2001. Methylation of histone H3 lysine 9 creates a binding site for HP1 proteins. Nature **410:**116–120.
30. **Lehming, N., A. Le Saux, J. Schuller, and M. Ptashne.** 1998. Chromatin components as part of a putative transcriptional repressing complex. Proc. Natl. Acad. Sci. USA **95:**7322–7326.
31. **Leinbach, S. S., and W. C. Summers.** 1980. The structure of herpes simplex virus type 1 DNA as probed by micrococcal nuclease digestion. J. Gen. Virol. **51:**45–59.
32. **Lentine, A. F., and S. L. Bachenheimer.** 1990. Intracellular organization of herpes simplex virus type 1 DNA assayed by staphylococcal nuclease sensitivity. Virus Res. **16:**275–292.
33. **Lomberk, G., L. Wallrath, and R. Urrutia.** 2006. The heterochromatin protein 1 family. Genome Biol. **7:**228.
34. **Lomonte, P., K. F. Sullivan, and R. D. Everett.** 2001. Degradation of nucleosome-associated centromeric histone H3-like protein CENP-A induced by herpes simplex virus type 1 protein ICP0. J. Biol. Chem. **276:**5829–5835.
35. **Lomonte, P., J. Thomas, P. Texier, C. Caron, S. Khochbin, and A. L. Epstein.** 2004. Functional interaction between class II histone deacetylases and ICP0 of herpes simplex virus type 1. J. Virol. **78:**6744–6757.
36. **Maul, G. G., and R. D. Everett.** 1994. The nuclear location of PML, a cellular member of the C3HC4 zinc-binding domain protein family, is rearranged during herpes simplex virus infection by the C3HC4 viral protein ICP0. J. Gen. Virol. **75:**1223–1233.
37. **Melroe, G. T., L. Silva, P. A. Schaffer, and D. M. Knipe.** 2007. Recruitment of activated IRF-3 and CBP/p300 to herpes simplex virus ICP0 nuclear foci: potential role in blocking IFN-beta induction. Virology **360:**305–321.
38. **Mossman, K. L., and J. R. Smiley.** 1999. Truncation of the C-terminal acidic transcriptional activation domain of herpes simplex virus VP16 renders expression of the immediate-early genes almost entirely dependent on ICP0. J. Virol. **73:**9726–9733.
39. **Muggeridge, M. I., and N. W. Fraser.** 1986. Chromosomal organization of the herpes simplex virus genome during acute infection of the mouse central nervous system. J. Virol. **59:**764–767.
40. **Nakayama, J., J. C. Rice, B. D. Strahl, C. D. Allis, and S. I. Grewal.** 2001. Role of histone H3 lysine 9 methylation in epigenetic control of heterochromatin assembly. Science **292:**110–113.
41. **Neumann, D. M., P. S. Bhattacharjee, N. V. Giordani, D. C. Bloom, and J. M. Hill.** 2007. In vivo changes in the patterns of chromatin structure associated with the latent herpes simplex virus type 1 genome in the mouse trigeminal ganglia can be detected at early times after butyrate treatment. J. Virol. **81:**13248–13253.
42. **Oh, J., and N. W. Fraser.** 2008. Temporal association of the herpes simplex virus genome with histone proteins during a lytic infection. J. Virol. **82:**3530–3537.
43. **Pinnoji, R. C., G. R. Bedadala, B. George, T. C. Holland, J. M. Hill, and S. C. Hsia.** 2007. Repressor element-1 silencing transcription factor/neuronal restrictive silencer factor (REST/NRSF) can regulate HSV-1 immediate-early transcription via histone modification. Virol. J. **4:**56.
44. **Pluta, A. F., W. C. Earnshaw, and I. G. Goldberg.** 1998. Interphase-specific association of intrinsic centromere protein CENP-C with HDaxx, a death

domain-binding protein implicated in Fas-mediated cell death. J. Cell Sci. **111:**2029–2041.
45. **Poon, A. P., Y. Liang, and B. Roizman.** 2003. Herpes simplex virus 1 gene expression is accelerated by inhibitors of histone deacetylases in rabbit skin cells infected with a mutant carrying a cDNA copy of the infected-cell protein no. 0. J. Virol. **77:**12671–12678.
46. **Preston, C. M., R. Mabbs, and M. J. Nicholl.** 1997. Construction and characterization of herpes simplex virus type 1 mutants with conditional defects in immediate early gene expression. Virology **229:**228–239.
47. **Preston, C. M., and M. J. Nicholl.** 1997. Repression of gene expression upon infection of cells with herpes simplex virus type 1 mutants impaired for immediate-early protein synthesis. J. Virol. **71:**7807–7813.
48. **Rice, J. C., and C. D. Allis.** 2001. Histone methylation versus histone acetylation: new insights into epigenetic regulation. Curr. Opin. Cell Biol. **13:** 263–273.
49. **Samaniego, L. A., L. Neiderhiser, and N. A. DeLuca.** 1998. Persistence and expression of the herpes simplex virus genome in the absence of immediate-early proteins. J. Virol. **72:**3307–3320.
50. **Samaniego, L. A., N. Wu, and N. A. DeLuca.** 1997. The herpes simplex virus immediate-early protein ICP0 affects transcription from the viral genome and infected-cell survival in the absence of ICP4 and ICP27. J. Virol. **71:** 4614–4625.
51. **Sampath, P., and N. A. Deluca.** 2008. Binding of ICP4, TATA-binding protein, and RNA polymerase II to herpes simplex virus type 1 immediate-early, early, and late promoters in virus-infected cells. J. Virol. **82:**2339–2349.
52. **Shahbazian, M. D., and M. Grunstein.** 2007. Functions of site-specific histone acetylation and deacetylation. Annu. Rev. Biochem. **76:**75–100.
53. **Shi, Y., F. Lan, C. Matson, P. Mulligan, J. R. Whetstine, P. A. Cole, R. A. Casero, and Y. Shi.** 2004. Histone demethylation mediated by the nuclear amine oxidase homolog LSD1. Cell **119:**941–953.
54. **Spivack, J. G., and N. W. Fraser.** 1988. Expression of herpes simplex virus type 1 (HSV-1) latency-associated transcripts and transcripts affected by the deletion in avirulent mutant HFEM: evidence for a new class of HSV-1 genes. J. Virol. **62:**3281–3287.
55. **Spivack, J. G., and N. W. Fraser.** 1988. Expression of herpes simplex virus type 1 latency-associated transcripts in the trigeminal ganglia of mice during acute infection and reactivation of latent infection. J. Virol. **62:**1479–1485.
56. **Stinski, M. F., and T. J. Roehr.** 1985. Activation of the major immediate early gene of human cytomegalovirus by *cis*-acting elements in the promoter-regulatory sequence and by virus-specific *trans*-acting components. J. Virol. **55:**431–441.
57. **Stinski, M. F., D. R. Thomsen, R. M. Stenberg, and L. C. Goldstein.** 1983. Organization and expression of the immediate early genes of human cytomegalovirus. J. Virol. **46:**1–14.
58. **Sullivan, K. F., M. Hechenberger, and K. Masri.** 1994. Human CENP-A contains a histone H3 related histone fold domain that is required for targeting to the centromere. J. Cell Biol. **127:**581–592.
59. **Terry-Allison, T., C. A. Smith, and N. A. DeLuca.** 2007. Relaxed repression of herpes simplex virus type 1 genomes in murine trigeminal neurons. J. Virol. **81:**12394–12405.
60. **Thomsen, D. R., R. M. Stenberg, W. F. Goins, and M. F. Stinski.** 1984. Promoter-regulatory region of the major immediate early gene of human cytomegalovirus. Proc. Natl. Acad. Sci. USA **81:**659–663.
61. **van Leeuwen, H., M. Okuwaki, R. Hong, D. Chakravarti, K. Nagata, and P. O'Hare.** 2003. Herpes simplex virus type 1 tegument protein VP22 interacts with TAF-I proteins and inhibits nucleosome assembly but not regulation of histone acetylation by INHAT. J. Gen. Virol. **84:**2501–2510.
62. **Verdin, E., F. Dequiedt, and H. G. Kasler.** 2003. Class II histone deacetylases: versatile regulators. Trends Genet. **19:**286–293.
63. **Wang, Q. Y., C. Zhou, K. E. Johnson, R. C. Colgrove, D. M. Coen, and D. M. Knipe.** 2005. Herpesviral latency-associated transcript gene promotes assembly of heterochromatin on viral lytic-gene promoters in latent infection. Proc. Natl. Acad. Sci. USA **102:**16055–16059.
64. **Zabierowski, S., and N. A. DeLuca.** 2004. Differential cellular requirements for activation of herpes simplex virus type 1 early (tk) and late (gC) promoters by ICP4. J. Virol. **78:**6162–6170.
65. **Zhang, Y., and C. Jones.** 2001. The bovine herpesvirus 1 immediate-early protein (bICP0) associates with histone deacetylase 1 to activate transcription. J. Virol. **75:**9571–9578.